Strain Birefringence of Kevlar* Aramid Fibers

H. H. YANG, M. P. CHOUINARD, and W. J. LINGG, *E. I. duPont de Nemours and Company, Inc., Richmond, Virginia 23261*

Synopsis

We have measured the strain birefringence of Kevlar aramid fibers under static loading via a spectrophotometric method. At very low strain rates, the birefringence of Kevlar fibers increases markedly with increasing strain. On initial straining, the birefringence increases even at relatively constant modulus. This is attributed to the orientation of macroscopic species in the fiber which were observed by visible light microscopy. Such behavior is supported by the experimental observation of laser diffraction patterns and optical transmission images of Kevlar fibers under load. In the final stage of straining where the fiber modulus increases rapidly, the birefringence increase is attributable to crystalline orientation. The spectrophotometric method is useful for the simultaneous measurement of stress, strain, and birefringence of highly oriented, highly crystalline fibers such as Kevlar aramid. It is particularly useful to study the morphological inhomogeneity of a fiber which is undetectable by the conventional tensile test.

INTRODUCTION

The characterization of synthetic fibers by stress–strain measurement is a well-known technique. To further study fiber structure–property relationships, more sophisticated methods are employed. This is particularly true with the high-performance Kevlar aramid fibers which provide high strength and high modulus via a highly oriented, highly crystalline rigid-chain structure. Although the stress–strain behavior of Kevlar fibers can be readily measured, their fiber birefringence is too high to be measured by conventional methods.

In a previous paper, we reported the development of a spectrophotometric method for measuring the birefringence of highly oriented fibers.[1] We have since extended this method to measure the stress, strain, and birefringence of a fiber simultaneously under varying load conditions. Such measurements have given some insights into the tensile behavior of Kevlar fibers under static load. This paper covers our extended experimental results of fiber birefringence under strain.

EXPERIMENTAL

Kevlar Aramid Fibers

Several samples of Kevlar continuous filament yarns were evaluated in this investigation. These yarns fell into two product types: Kevlar and Kevlar 49.

*Kevlar is a registered trademark of E. I. du Pont de Nemours and Co., Inc.

Journal of Applied Polymer Science, Vol. 34, 1399–1414 (1987)
 CCC 0021-8995/87/041399-16$04.00

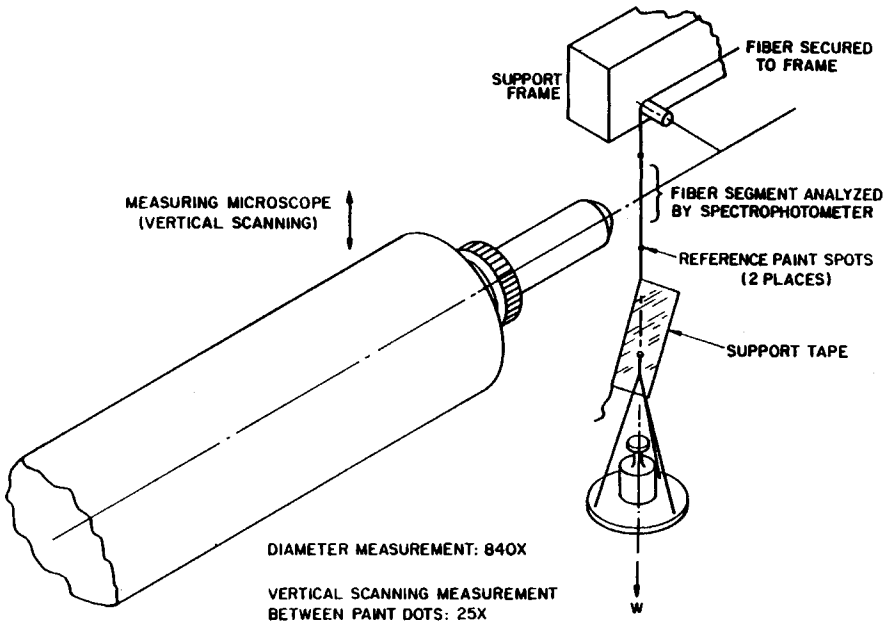

Fig. 1. Fiber diameter and scanning microscope arrangement.

Kevlar 49 fibers have a considerably higher degree of crystalline orientation and higher modulus than Kevlar fibers. In addition, these fibers differ in yarn and filament deniers, where denier is the fiber weight (g) of 9000 m length. Most Kevlar yarns contain 1.5 and 2.25 dpf (denier per filament) fibers. The nominal fiber diameters are 12 and 14.7 μm, respectively.

To prepare for our birefringence measurement, a 15-cm long filament section was first cut from the yarn sample. The single filament was gently pulled from the yarn bundle. It was then inspected by an optical microscope to ensure that it was free of physical damages. The fiber specimen would be rejected if physical damages were detected. As a rule, at least duplicate measurements were made for each yarn sample. The reproducibility of both strain and birefringence measurements was within $\pm 5\%$ in our experience, unless a gross interfilament nonuniformity existed in the yarn sample.

Static Birefringence Measurement

The stress–strain and birefringence values for Kevlar aramid fibers were measured under static loading conditions. The experimental procedure is described below.

Figures 1 and 2 illustrate diagramatically the experimental arrangement for static birefringence measurements under ambient conditions. A single filament specimen was hung from a specially designed support frame. It was kept straight by attaching a pan weighing 1 g. This stress was relatively low for aramid fibers and caused essentially no extension of the fiber specimen. A vertical scanning optical microscope with built-in calibrated reticle and 840 $\times$ magnification was used to measure the fiber diameter. The fiber length was also measured via the microscope's vernier scale at 25 $\times$ between two paint

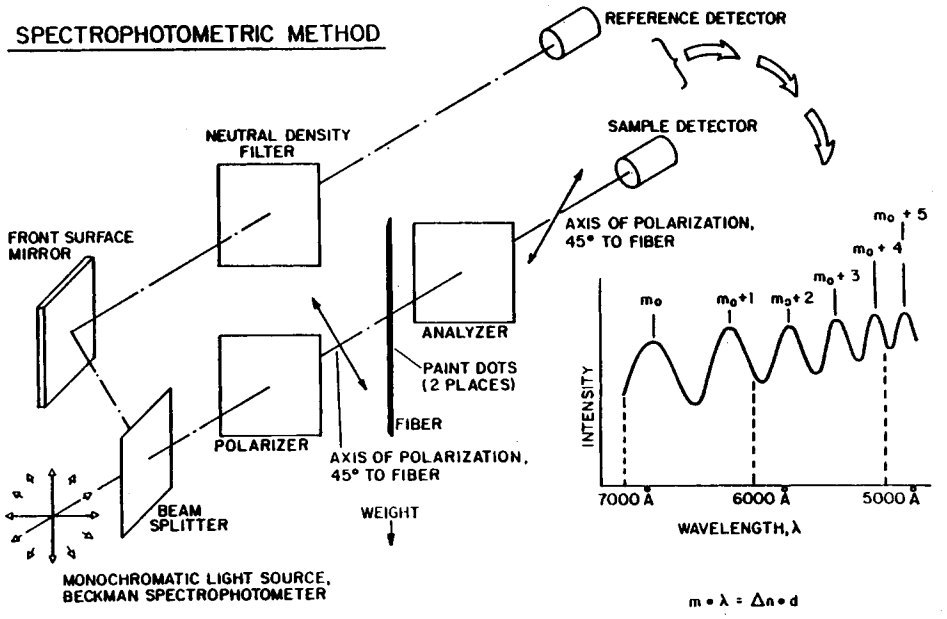

Fig. 2. Arrangement for optical retardation measurement.

spots on the fiber. These paint spots were approximately 1 cm apart. They were so selected that the Beckman Spectrophotometer beam would pass between them. The use of paint dots further eliminated the need to determine any slippage that might occur in the support system during the loading experiment. The accuracy of fiber length measurement between the paint dots by this procedure was 0.1 mm, with 1% precision.

The fiber birefringence was measured with the optical arrangement shown in Figure 2 at 90° to the diameter measurement arrangement in Figure 1. The weighted fiber specimen was placed in the sample chamber of a dual beam Beckman spectrophotometer ACTA MVII. The spectrophotometer employed two light beams, one reference and the other the sample beam. The sample beam was modified with the polarizer and analyzer with the filament between them. The transmitted light was compared to the reference beam and the result displayed on a recording chart. As the Beckman unit scanned the visible spectrum, the intensity pattern for the transmitted light varied accordingly. The variation in intensity permits the calculation of birefringence according to the following equation:[1]

$$m\lambda = d\Delta n \tag{1}$$

Therefore,

$$\Delta n = m\lambda/d \tag{2}$$

where Δn is the birefringence, λ is the wavelength, d is the fiber diameter, and m is an integer. In the present investigation, we have arbitrarily chosen $m = 1, 2, 3 \ldots$ for the light intensity peaks, and $\lambda = 6000$ Å for the evaluation of Δn. For example, the peaks in Figure 2 are numbered consecutively between 7000 and 5000 Å.

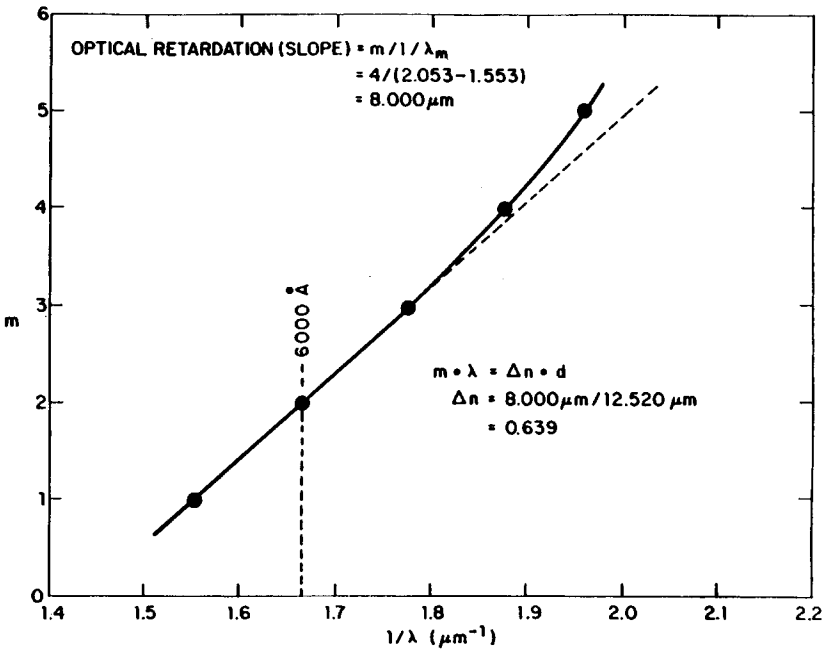

Fig. 3. Graphical solution for determining optical retardation and birefringence. Sample: Kevlar® aramid fiber.

Figure 3 illustrates a plot of m vs. $1/\lambda$ for a 1.5 denier Kevlar fiber at 1 g load. The slope of the tangent line to the curve at 6000 Å, which is determined graphically from $\Delta m/\Delta(1/\lambda)$, gives the optical retardation $m\lambda$. We chose the wavelength of 6000 Å for the slope determination because the curve is generally most linear in this region. The arbitrary integer designation of m values does not affect the value of optical retardation because Δm is determined from differential change and is not affected by absolute m values. The same result would be obtained if the minimum intensity peaks (valleys) were used.

The fiber birefringence was then calculated for eq. (2). Thus, from Figure 3, at $\lambda = 6000$ Å,

$$d\Delta n = 8.000\ \mu m$$

Since $d = 12.52$ μm from average microscopic reading,

$$\Delta n = m\lambda/d = 8.000/12.52 = 0.639$$

This Δn value is the fiber birefringence at 1 g static load. The above procedure was then repeated as the load on the fiber specimen was incrementally increased. At each load increase, simultaneous measurements of stress, strain, and birefringence were made. For convenience, the stress was expressed in grams per denier (gpd), and strain in % elongation. The birefringence of a strained fiber was called strain birefringence.

The experimental time for each measurement of strain birefringence at a given load was approximately 10 min. This amounted to about 1.5 h of total

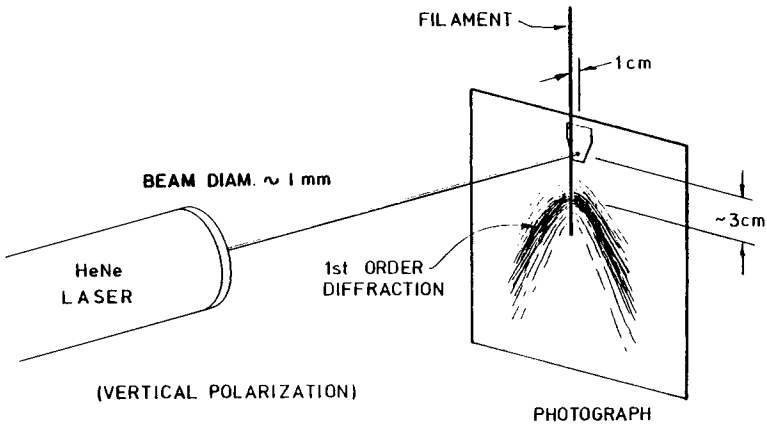

Fig. 4. Laser diffraction arrangement.

experimental time for eight incremental loadings on a single filament. In supplementary experiments, we found that the fiber deformation observed in each static loading achieve 90–95% that of long-term creep. Therefore, we can consider our static loading experiments to be at a very low strain rate.

Laser Diffraction

Figure 4 shows the experimental arrangement for laser diffraction. A He–Ne laser source, vertically polarized, with 1 mm beam diameter was directed at a fiber specimen. The light scattering from the fiber produced an effect that is similar to the optical diffraction from multiple gratings. A photographic film with the emulsion side precisely 1 cm from the fiber was used to record the laser diffraction pattern. In order to obtain the best photographic quality, the zero order (laser source) was blocked at the film plane to reduce its burning and light scattering. All photographs were exposed to equal laser intensity for the same length of time.

The laser diffraction pattern can be used to compute the substructural spacing in a fiber according to:

$$m(\lambda/n) = D \sin\theta \tag{3}$$

Therefore,

$$D = m\lambda/(n \sin\theta) \tag{4}$$

where D is the spacing (Å), m is 1 for the first order of diffraction with maximum intensity, λ is 6328 Å, wavelength of the laser source, n is 1.62, the refractive index of Kevlar fibers; and θ is the angle between the first-order diffraction pattern on the photograph and the laser beam.

Optical Microscopy

Conventional optical microscopy in a cross-polarized light field was used to study the fibe morphology. A microscopic observation of Kevlar fiber under load was made with optical microscope by Dr. E. J. Roche, Central Research and Development Department, Du Pont Co., Wilmington DE.

RESULTS

Strain Birefringence

Table I presents results from a series of simultaneous stress, strain, and birefringence measurements on a 1.5 dpf Kevlar aramid fiber. These results can be readily plotted as stress–strain and birefringence–strain curves in Figure 5. The most significant phenomenon is that the fiber birefringence increases markedly with strain. The birefringence increase persists until the fiber ultimately breaks. The stress–strain behavior is also interesting. In some cases, the stress–strain curve is nonlinear. This is surprising since Kevlar fibers generally exhibit linear stress–strain relationships at relatively high strain rates in conventional tensile test.[2] However, some Kevlar fibers did

TABLE I
Static Loading of Kevlar Fibers[a]

Wt on Fiber (g)	Avg fiber diam (μm)	Stress (gpd)	Fiber length (mm)	Strain (% elong.)	Birefringence
1	12.5	0.63	18.87	0	0.639
6	12.4	3.83	19.05	0.9	0.742
11	12.3	7.16	19.13	1.4	0.771
16	12.3	10.42	19.20	1.8	0.784
21	12.3	13.67	19.25	2.0	0.797
26	12.3	16.93	19.30	2.3	0.804
31	12.3	20.18	19.37	2.6	0.814
36	Broke				

[a]Sample: 1500 denier Kevlar aramid fiber.

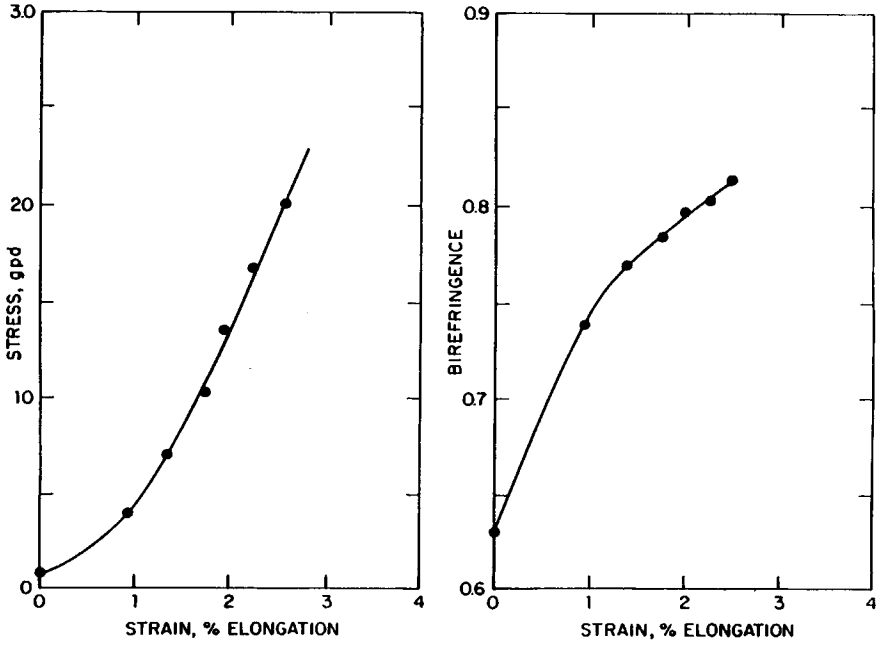

Fig. 5. 1.5 dpf Kevlar® aramid fiber under static load.

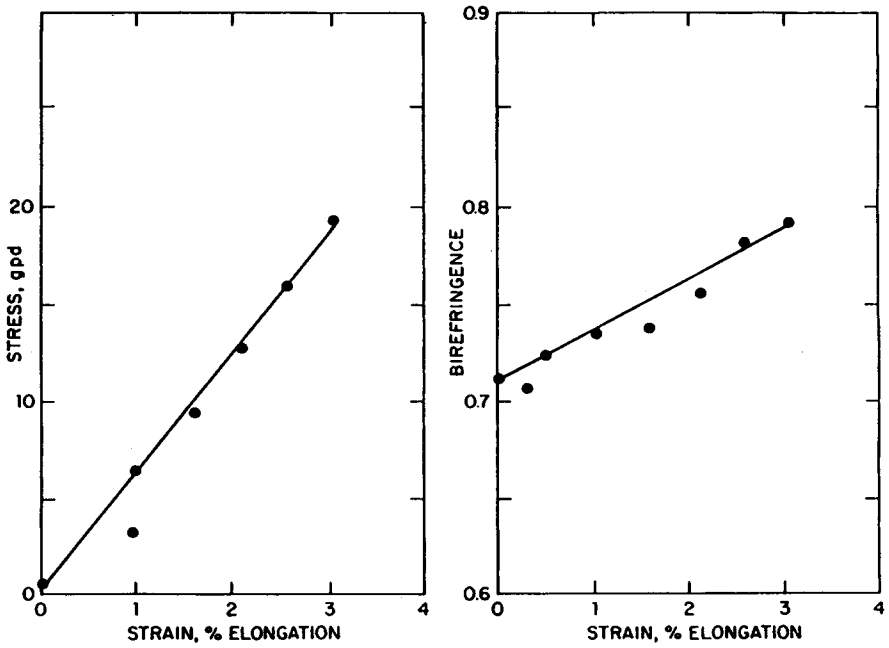

Fig. 6. 1.5 dpf Kevlar® aramid fiber under static load.

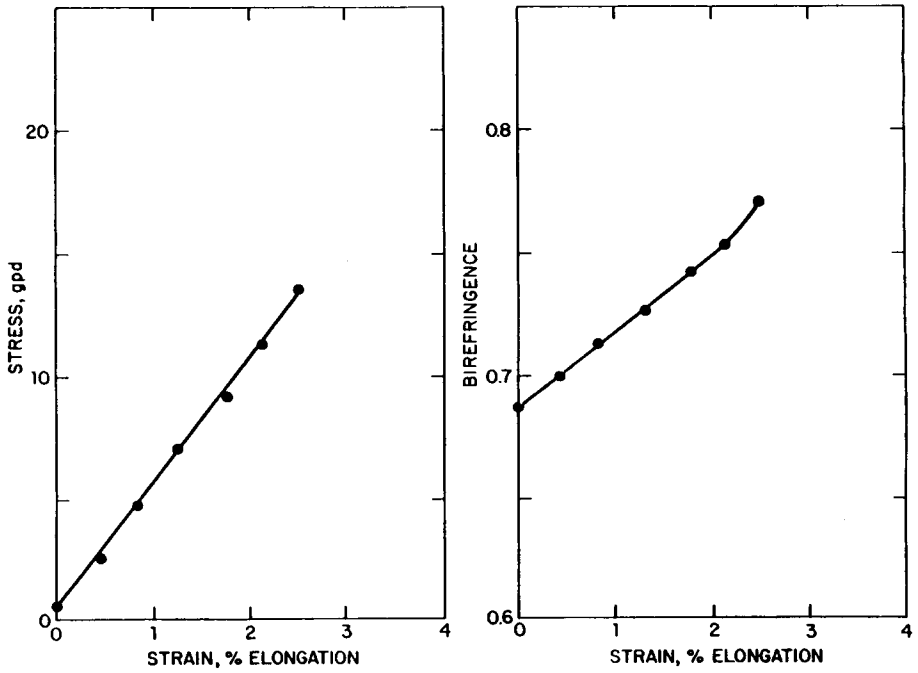

Fig. 7. 2.25 dpf Kevlar® aramid fiber under static load.

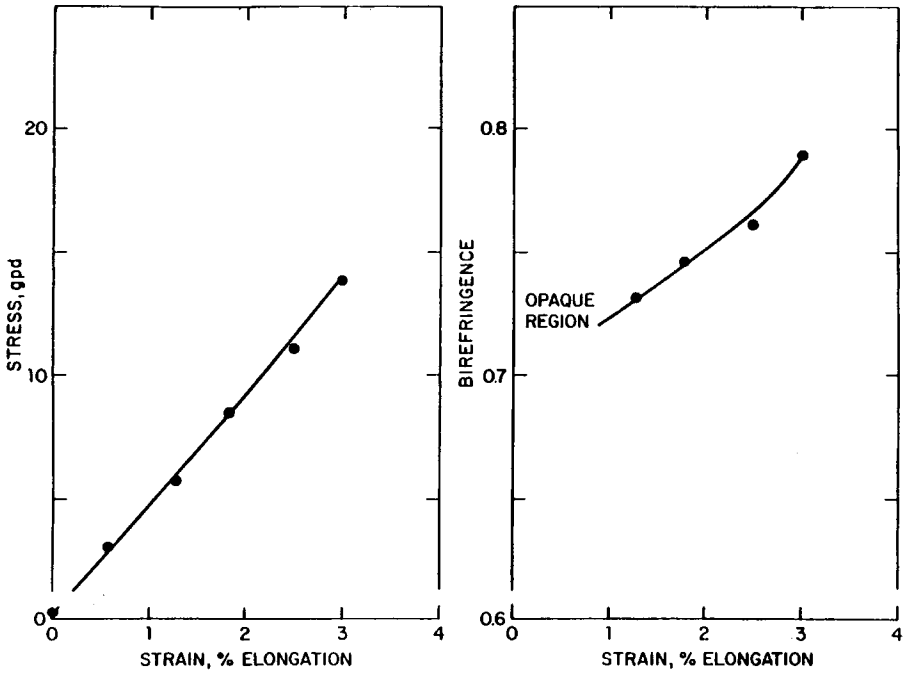

Fig. 8. Defective 3.0 dpf Kevlar® aramid fiber under static load.

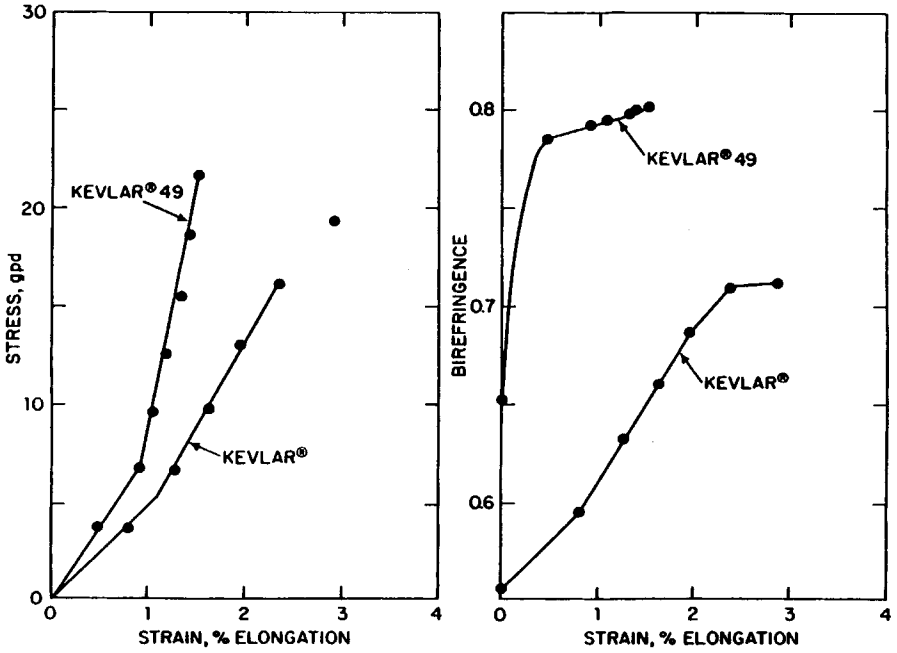

Fig. 9. Kevlar® and Kevlar® 49 aramid fibers under static load.

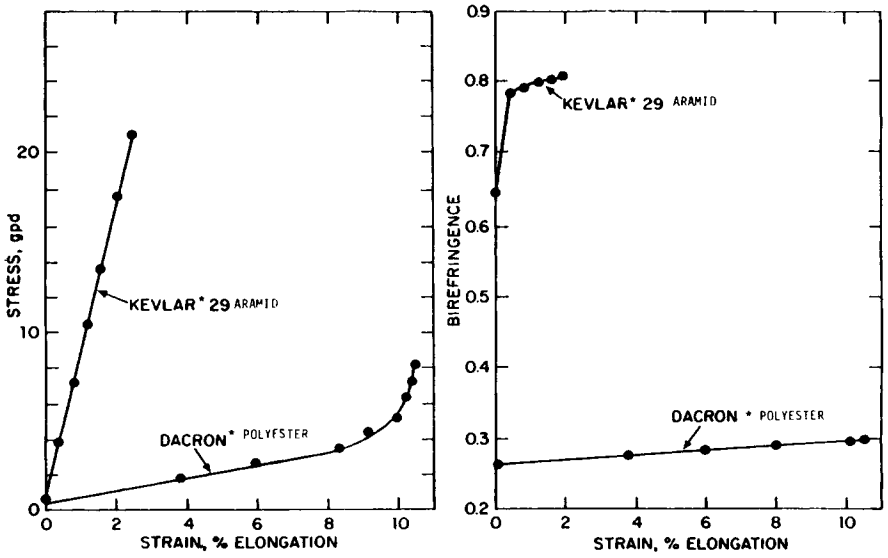

Fig. 10. Kevlar® vs. Dacron® fibers under static load.

exhibit near-linear stress–strain curves and their birefringence–strain curves closely tracked the near-linearity. This behavior is illustrated in Figure 6. As a group, fibers with near-linear behavior generally have higher initial modulus than those with nonlinear behavior.

Figures 7 and 8 show the stress–strain and birefringence–strain curves of experimental 2.25 and 3.0 dpf Kevlar fibers, respectively. Both of these fibers gave lower initial modulus and birefringence values than the 1.5 dpf Kevlar fiber in Figure 5. More interestingly, the 3.0 dpf fiber was optically opaque at $< 1\%$ strain. Its stress–strain curve, however, gave no indication of unusual behavior.

Figure 9 presents the stress–strain and birefringence–strain curves of a Kevlar 49 fiber. It can be seen that the Kevlar 49 fiber exhibits higher initial modulus and higher birefringence than all other Kevlar fibers. When the fiber was strained, the birefringence first increased very rapidly from 0.65 to 0.78. It then slowed down abruptly at 0.5% strain and reached a final value of 0.80 shortly before fiber break. At the same time, the stress–strain curve exhibited a modulus increase beyond 0.5% strain and reached very high modulus (> 1500 gpd) before fiber break.

For comparison to Kevlar fibers, the stress, strain, and birefringence of a Dacron† polyester fiber were measured. Figure 10 shows that the Dacron fiber had a low birefringence value of 0.25 at zero strain and gave very small birefringence response to strain. These observations are significantly different from those of Kevlar fibers.

Laser Diffraction Pattern

Figure 11 compares the laser diffraction patterns of Kevlar, Kevlar 49, and Dacron fibers. With the experimental arrangement given in Figure 4, Kevlar

†Dacron is a registered trademark of E. I. du Pont de Nemours and Co., Inc.

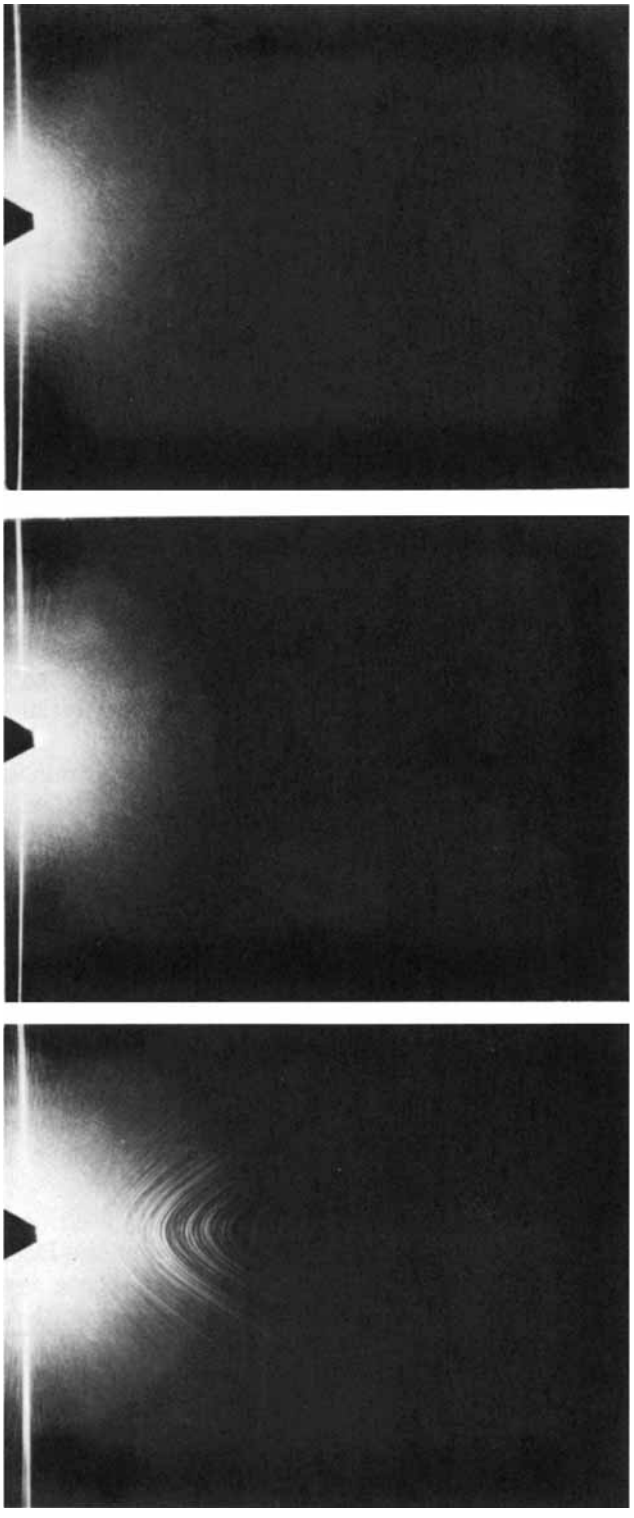

Fig. 11. Laser diffraction patterns of various fibers.

fiber produced a distinct diffraction pattern that enabled us to compute the substructural spacing D according to eq. (4). The first-order scattering of maximum intensity was 3 cm below the zero order. At 1-cm distance between the fiber and the photographic emulsion, this yields an angle θ of 71.6° and hence spacing D of 4117 Å. This is approximately two-thirds of the wavelength of light beam which is 6000 Å. Thus we may attribute the laser diffraction to the optical activity of a macroscopic structure in Kevlar fibers.

The diffraction pattern of Kevlar 49 fiber is different from that of Kevlar fiber. Figure 11(b) shows only a faint hint of diffraction, which suggests

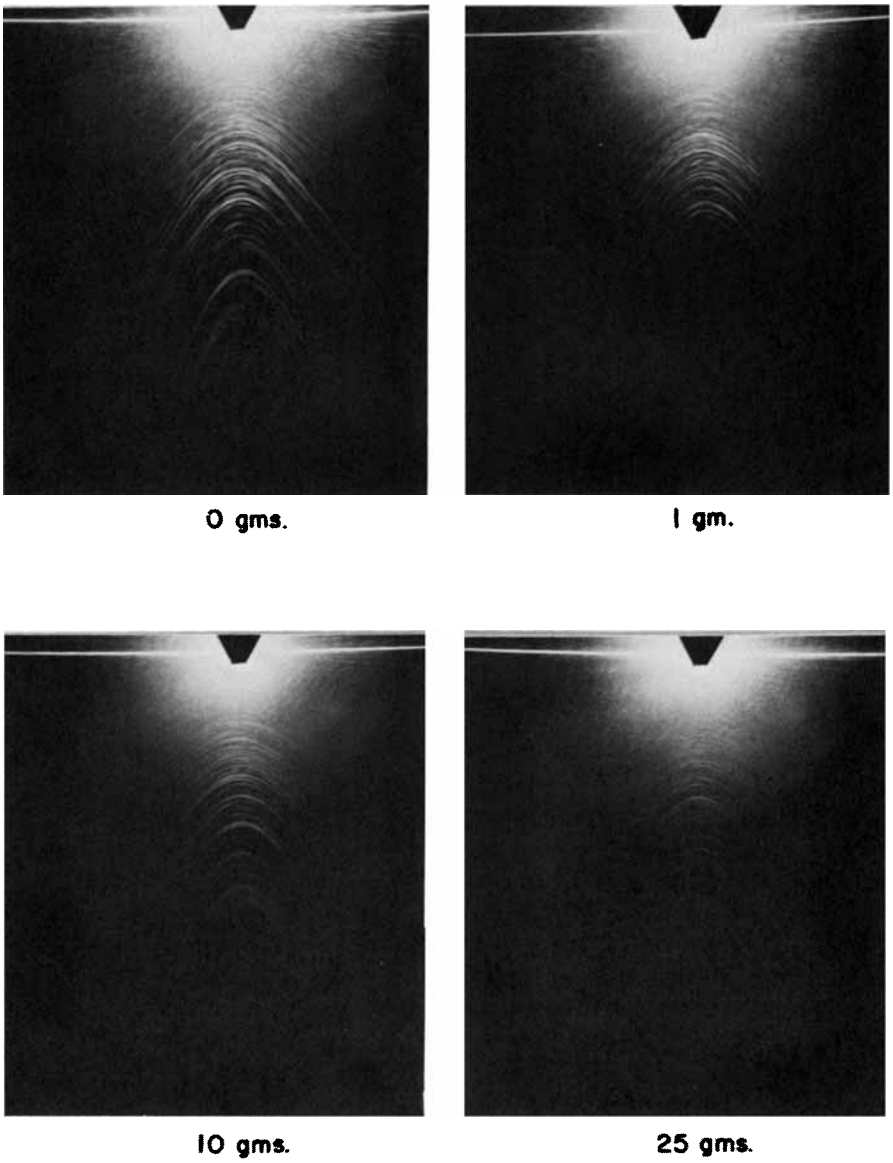

Fig. 12. Laser diffraction patterns of Kevlar® fiber under increasing strain.

significant modifications of the macroscopic structure in Kevlar 49 fiber. In comparison, Dacron fiber showed no diffraction pattern at all. This can be simply attributed to the absence of a macroscopic periodicity in Dacron fibers.

Figure 12 displays the first-order patterns for a series of static loading experiments. When the Kevlar fiber was increasingly strained, the diffraction pattern diminished progressively. When the fiber was relaxed, the diffraction pattern returned. This indicates the elastic recovery of a macroscopic structure in Kevlar fiber during loading and unloading.

Optical Microscopy

It is well known that Kevlar fibers have a transverse pleat structure at a periodicity of 5000–6000 Å.[3] This is illustrated in the optical micrograph of a 1.5 dpf Kevlar fiber in Figure 13. When a load of 30 g (20 g per denier) was

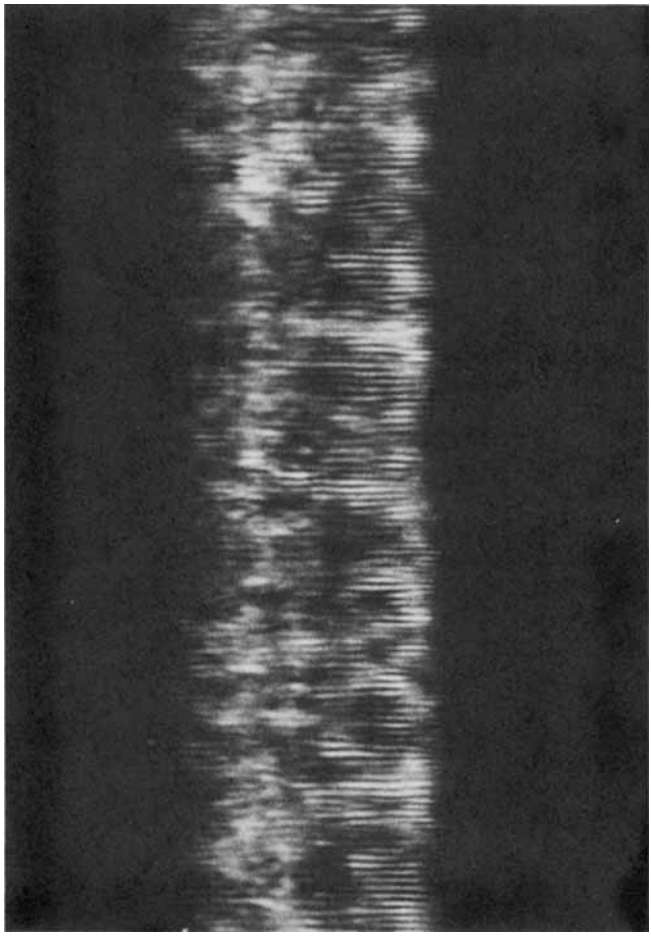

(a)

Fig. 13. Optical micrographs of 15-dpf Kevlar® filament: (a) at no load, fiber shows a transverse pleat structure; (b) at 30 g load, the transverse pleat structure has greatly diminished.

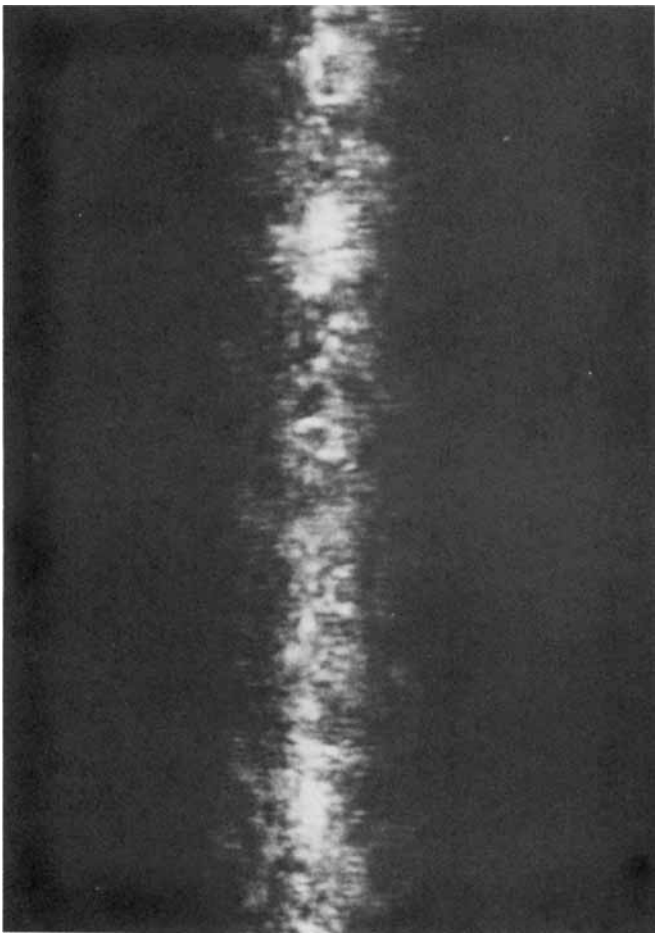

(b)

Fig. 13. (*Continued from the previous page.*)

applied to the fiber, the transverse pleat structure diminished greatly except a faint suggestion in the fiber core.

DISCUSSION

Stress–Strain–Birefringence Relationship

Since the fiber deformation in our static loading experiments was conducted manually, we can readily consider each incremental loading as a step process at low strain rate. Therefore, the deformation process differs from the conventional tensile test at relatively high strain rates. We believe that, at slow strain rate, the fiber has enough time to respond through structural rearrangements. Such response may be only partially possible at high strain rates. For this reason, Kevlar fibers generally exhibit high modulus, particularly near the break point in the static loading experiment than in the conventional tensile test.

A careful study of Figures 4–7 will show that the birefringence–strain curve of Kevlar fiber tracks the stress–strain curve. The birefringence increases rapidly even through the fiber modulus is relatively constant in the initial stage of straining. In the final stage of straining, birefringence tends to plateau out as modulus approaches very high values. Although the strain-induced birefringence increase of Kevlar fibers is not unique as compared to the conventional fibers, its structural significance is quite interesting. With conventional fibers, an increase in birefringence results from increasing crystallinity and crystal orientation. However, the birefringence increase with the increasing strain for both Kevlar 49 and Kevlar fibers must be attributed to the combined contribution of microscopic and macroscopic structural changes. In the initial stage of fiber straining, the birefringence increases even at a relatively constant modulus. This birefringence increase coincides with the changes in the laser diffraction pattern and optical transmission images. Thus, we can attribute these changes largely to the orientation of macroscopic species in the fiber. These species are of a visible dimension (e.g., 3000–6000 Å) detectable by the polarized light and laser beams. Morphologically, this scale is on the order of fibril size and pleat spacing in Kevlar fibers. In the final stage of fiber straining where the modulus increases rapidly, the birefringence increase results predominantly from crystal orientation in a highly crystalline fiber.

The structural rearrangement which takes place in the initial stage of straining suggests some kind of inhomogeneity in Kevlar fibers. This is especially evident in Figure 6 where the 3.0 dpf Kevlar fiber exhibited optical opacity in initial straining. In that case, the inhomogeneity might be in the form of skin/core orientation gradient due to relatively large fiber diameter. This inhomogeneity was quickly dissipated in initial straining largely from morphological movements in the fiber.

Modulus–Birefringence Relationship

The birefringence value at zero strain and the rate of birefringence change with strain for Kevlar fibers, as seen in Figures 5–7, track the fiber modulus

TABLE II
Strain Birefringence vs. Initial Modulus

Fiber type	Strain birefringence Δ_n (0.5%)	Initial modulus M_i (gpd)
Kevlar 49	0.79	750
Kevlar	0.58	500
Kevlar	0.765	633
Kevlar	0.63	553
Kevlar	0.625	537
Kevlar 49	0.73	770
Kevlar	0.67	620
Kevlar	0.755	840
Kevlar	0.71	840
Kevlar	0.705	550
Kevlar	0.705	650
Dacron	0.25	40

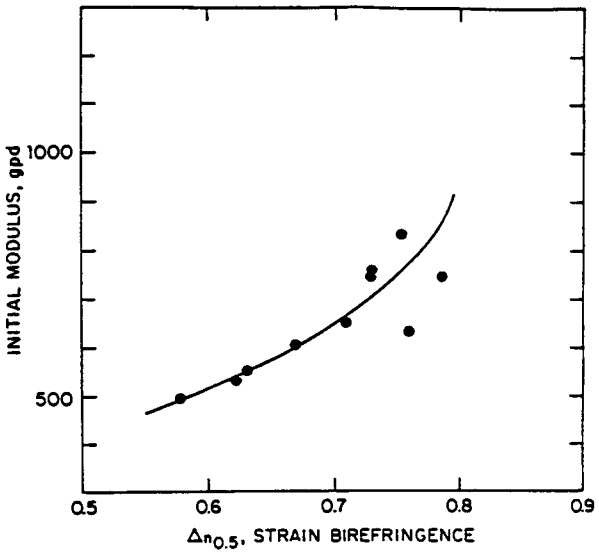

Fig. 14. Modulus vs. strain birefringence.

closely. In seeking a simple relationship, we have chosen the strain birefringence at 0.5% strain as a structural parameter. Table II presents the strain birefringence and initial modulus of several widely different Kevlar aramid fibers.

An empirical correlation of these parameters is given in Figure 14. The correlation, although with some scatter, shows that strain birefringence increases with increasing modulus. Based on this, we may consider strain birefringence as indicative of the degree of crystal orientation in Kevlar fibers.

CONCLUSION

The major finding from our simultaneous stress–strain–birefringence measurements of Kevlar fibers is the birefringence increase with strain even at relatively constant fiber modulus. We have interpreted the birefringence increase in terms of structural changes and crystal orientation. We have also attempted to support our interpretation with the results of laser scattering and strain-optical microscopy.

We believe that the basic principles of our stress–strain–birefringence measurement are sound. The birefringence value obtainable with this method is the bulk-average birefringence across a fiber diameter and is accurate to 0.05. The method is useful to study the tensile behavior of a fiber at relatively low strain rates. More importantly, the birefringence–strain information can be used to study the structural inhomogeneity of a fiber which is undetectable by the conventional tensile test.

The experimental method in its present form is elegant but tedious. We are very hopeful that it can be automated with electronic sensing and digital computation.

References

1. H. H. Yang, M. P. Chouinard, and W. J. Lingg, *J. Polym. Sci., Polym. Phys. Ed.*, **20**, 981 (1982).

2. W. E. Morton and J. W. S. Hearle, *Physical Properties of Textile Fibers*, Butterworths, London, 1962.

3. M. Panar, P. Avakian, R. C. Blume, K. H. Gardner, T. D. Gierke, and H. H. Yang, *J. Polym. Sci., Polym. Phys. Ed.*, **21**, 1955 (1983).

Received August 30, 1986
Accepted March 13, 1987